ELSEVIER

Journal of Chromatography A, 777 (1997) 177–192

JOURNAL OF CHROMATOGRAPHY A

Determination of mono- and disulphonated azo dyes by liquid chromatography–atmospheric pressure ionization mass spectrometry

Clara Ràfols[a], Damià Barceló[b,*]

[a]*Department of Analytical Chemistry, Universitat de Barcelona, Diagonal 647, 08028 Barcelona, Spain*
[b]*Department of Environmental Chemistry, CID-CSIC, c/Jordi Girona, 18-26, 08034 Barcelona, Spain*

Abstract

Liquid chromatography–atmospheric pressure chemical ionization (APCI) mass spectrometry (MS) with positive (PI) and negative (NI) modes of operation and liquid chromatography–high flow pneumatically assisted electrospray (ES) mass spectrometry with negative mode were used for the determination of the disulphonated azo dyes Acid Red 1, Mordant Red 9, Acid Red 13, Acid Red 14, Acid Red 73, Acid Yellow 23, Direct Yellow 28 and Acid Blue 113 and of the monosulphonated azo dyes Mordant Yellow 8, Mordant Black 11 and Mordant Black 17. High fragmentation was observed when using APCI with losses of one or two SO_3Na groups, either attached to one ring or two different rings. Losses of Na and 2Na are common to all techniques used. High flow ES was the most sensitive technique for all the dyes studied, except for Mordant Red 9, with a linear range varying from 1–3 to 700–800 ng. APCI using negative ion mode was one order of magnitude less sensitive than ES, with a linear range varying from 50–70 to 2000–3000 ng, whereas positive ion mode APCI-MS showed the poorest linear range and sensitivity. The determination of Direct Yellow 28 and Acid Blue 113 in water samples was also reported by preconcentrating 500 ml of water with solid-phase disk extraction followed by LC–high flow pneumatically assisted ES-MS. © 1997 Elsevier Science B.V.

Keywords: Dyes; Azo dyes, sulphonated

1. Introduction

According to recent information [1], world dye production rose by more than 10% annually to 2.2 billion lbs. in 1994 (1 lb.=0.4536 kg). The value of the dyes used rose by just more than 10% annually to US$9.2 billion. The numbers for 1995 are not yet available. The textile industry is the largest consumer of these products, accounting for two-thirds of the dyestuff market [2]. Recent estimates indicate that approximately 12% of the synthetic textile dyes used each year are lost to waste water during manufacturing and processing operations and that 20% of those losses will enter the environment through effluents from waste water treatment plants. Of the dyes available on the market today, approximately 50% are azo compounds. Azo dyes can be divided into monoazo, diazo and triazo classes and are found in various categories, i.e., acid, basic, direct, disperse, azoic and pigments. Of the various categories, acid and premetalized dyes account for 12%.

Disulphonated azo dyes represent major problems in drinking water plants in Spain and two papers have been published where these compounds were analyzed by fast atom bombardment [3,4].

Thermospray LC–MS and LC–MS–MS have been extensively used for the determination of azo dyes, mainly monosulphonated azo dyes [5–10]. Few papers have been published that have used atmospheric pressure ionization (API) techniques, under

*Corresponding author.

PII S0021-9673(97)00429-9

negative ion mode (NI) MS [8,11–14]. Most of these papers used NI electrospray MS (conventional electrospray) with an eluent flow-rate of a few μl/min and were mainly applied to monosulphonated azo dyes, such as Acid Orange 7, Acid Red 88 and 151 and others [14]. To our knowledge, PI mode has not been used to date for the determination of these types of dyes.

It has been pointed out that disulphonated azo dyes are more difficult to analyze than monosulphonated azo dyes by LC–MS. Usually, gas-phase ionization, using heated pneumatic nebulizer API, showed 20–50 times less sensitivity for disulphonated azo dyes than for monosulphonated azo dyes [14]. Until now, only a few disulphonated azo dyes were characterized by LC–API-MS techniques, including Acid Red 1, Acid Black 1, Acid Blue 113, Acid Yellow 23, Acid Red 14, Acid Red 18 and Acid Orange 10 [8,11,12,14]. The various approaches published for the determination of sulphonated dyes discussed aspects like fragmentation, sensitivity with various techniques, such as APCI or ES, and limits of detection. In order to perform quantitative analysis of dyes, it would be of interest to investigate the linear calibration range of these compounds using various interfacing systems and to determine the limits of detection and/or quantitation of a variety of dyes that are traditionally difficult to analyze by LC–MS techniques. This has not been performed until now for this type of compounds. Recently [15,16], we reported the use of high flow pneumatically assisted ES under PI and NI for the determination of various pesticides, with their corresponding calibration graphs and linearity. More recently [17], we reported data on the calibration and limits of detection for a variety of polar organophosphorus pesticides under PI and NI APCI-MS. In view of the previous work from our group [15–17] and, in the same way, on the determination of polysulphonated dyes by LC–MS, the objectives of this work are as follows: (i) To investigate the determination of a selection of polysulphonated azo dyes by LC–APCI-MS techniques using both high flow pneumatically assisted electrospray, which has never been used for the characterization of such types of dyes, and PI and NI APCI-MS (PI APCI-MS has not been used for this purpose and it can provide complementary structural information); (ii) to determine the linearity range and calibration data for all of the selected dyes using various modes of the LC–API-MS technique and (iii) to determine the concentration of a selection of dyes in water samples after solid-phase extraction.

The selection of dyes included eight disulphonated azo dyes that have previously been difficult to determine using LC–API-MS techniques and many that have never been investigated, such as Mordant Red 9, Acid Red 13, Acid Red 73, Direct Yellow 28 and the monosulphonated azo dyes Mordant Black 11, Mordant Black 17 and Mordant Yellow 8. The choice of dyes to analyze was based on their use in the area of Spain where they have been causing problems [3,4].

2. Experimental

2.1. Chemicals

HPLC-grade water and methanol for chromatography were obtained from Merck (Darmstadt, Germany). The solvents were passed through a 0.45-μm filter from Scharlau (Barcelona, Spain) before use. Ammonium acetate was purchased from Merck.

Azo and diazo commercial dyes were generously provided by ICI, Ciba-Geigy and Hoechst (Barcelona, Spain), following previous studies by colleagues in Barcelona [3,4]. Fig. 1 gives their Colour Index [18], name, chemical structure and molecular masses.

2.2. LC–MS

2.2.1. Thermospray (TS)

A Hewlett-Packard (Palo Alto, CA, USA) Model 5988A Thermospray LC–MS quadrupole mass spectrometer and a Hewlett-Packard Model 35741B instrument for data acquisition and processing were employed.

The characterization of sulphonated azo dyes was done in flow injection mode at 1 ml/min. Mixtures of 0.03 *M* aqueous ammonium acetate–methanol (50:50, v/v) served as the mobile phase and the optimized parameters are shown in Table 1.

2.2.2. Electrospray (ES)

A VG Platform ESP from Micromass (Manchester,

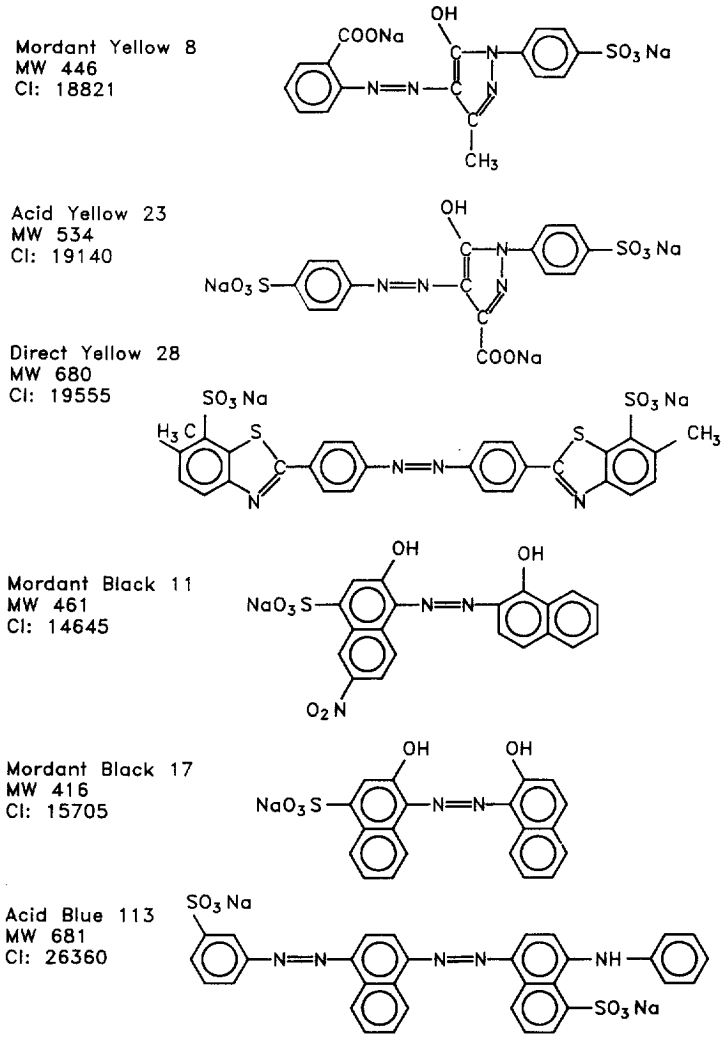

Fig. 1. (*continued on p. 180*)

UK), equipped with a Megaflow ES, was used. The instrument control and data processing involved the use of MassLynx software installed in a Digital DEC PC 466. A detailed description of the system is given elsewhere [15]. Table 1 shows the parameters used with this technique.

Flow injection analysis was carried out using 0.001 *M* aqueous ammonium acetate–methanol (50:50, v/v) at a flow-rate of 0.3 ml/min.

A 300×2.1 mm C_{18} column from Waters (Milford, MA, USA) was used for separation at a flow-rate of 0.3 ml/min. The eluents were 0.001 *M* aqueous ammonium acetate and methanol and the gradient elution programme used is shown in Table 2.

2.2.3. APCI

A VG platform from Micromass, equipped with a standard API source was used (for more details see reference [17]). The conditions used for APCI experiments are shown in Table 1.

Flow injection analysis were performed at 1 ml/min in 0.03 *M* aqueous ammonium acetate–methanol (50:50, v/v).

A 250×4.6 mm I.D column, packed with 5 μm Supelcosil LC-PCN, from Supelco, was used for the

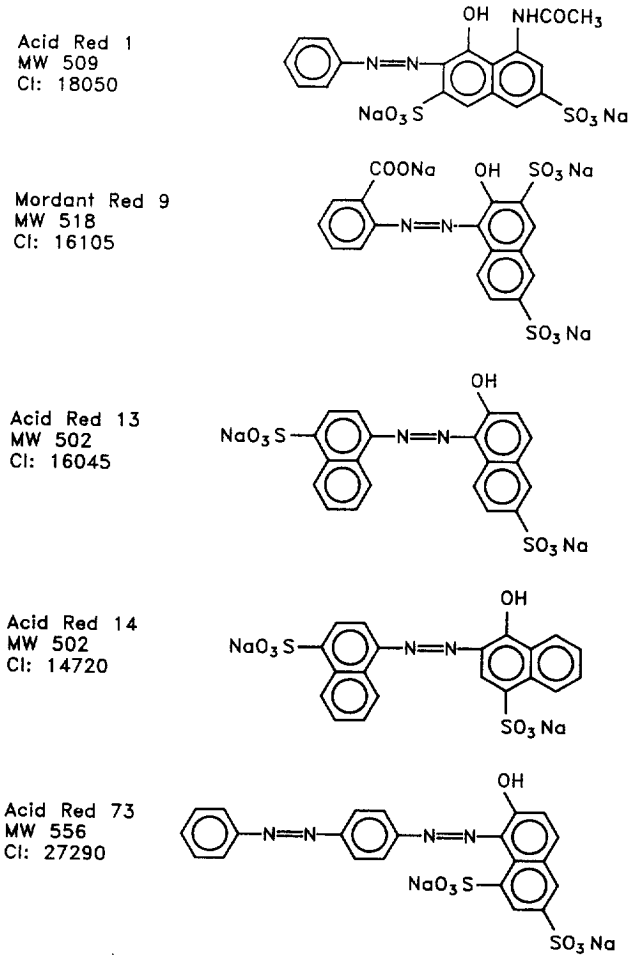

Fig. 1. Chemical structures of the dyes studied. MW=Molecular mass.

chromatographic separation. For this column, the LC eluent conditions varied from 10:90 (v/v) methanol–0.03 *M* aqueous ammonium acetate (10 min isocratic conditions) to 60:40 (v/v) methanol–0.03 *M* aqueous ammonium acetate over 15 min at a flow-rate of 0.9 ml/min.

2.3. Sample preparation and quantitation

All dyes were dissolved in water. Solutions containing 200, 100 and 50 ppm of dye were prepared for working in full-scan mode with TS, APCI and ES, respectively. In each case, 20 μl of dye were injected.

The linearity of the system was studied at twelve points (from 0.06 to 600 ng) using NI mode for ES and at ten points (from 10 to 2000 ng) using NI and PI mode for APCI and with time-scheduled SIM in each case. The ions selected for quantitation are listed in Table 3 and the calibration data are shown in Tables 4–6. Limits of detection (LODs) and limits of quantitation (LOQs) are also indicated in these tables. LODs were calculated by injecting diluted solutions containing the low levels of the dyes, with a signal-to-noise ratio of three–four (the ration between the peak intensity with SIM conditions and the noise). The LOQs were calculated from LODs, being 2.5–4 times greater than the LODs. Fig. 2

Table 1
Optimization of the different operating parameters

Technique	Parameter	Optimization conditions
LC–TS-MS	Flow-rate	1 ml/min
	Eluent	CH_3OH–water (50:50, v/v)+NH_4Ac (0.034 *M*)
	Source temperature	300°C
	Stem temperature	140°C
	Tip temperature	260°C
LC–ES-MS	Flow-rate	0.3 ml/min
	Eluent	CH_3OH–water (50:50, v/v)+NH_4Ac (0.001 *M*)
	Drying gas flow-rate	200 l/h
	ESI nebulizing gas flow	10 l/h
	Electrospray voltage	2.8 kV (2–3.5 kV)
	HV lens voltage	0.1 kV
	Extraction voltage	20 V (20–130 V)
	Focus voltage	27, 47 V
	Source temperature	150°C
LC–APCI-MS	Flow-rate	1 ml/min
	Eluent	CH_3OH–water (50:50, v/v) NH_4Ac (0.03 *M*)
	Drying gas flow-rate	400 l/h
	Nebulizing gas flow	50 l/h
	APCI voltage	2.5 kV
	Cone voltage	15 V
	Source temperature	180°C
	APCI probe temperature	500–600°C

shows the separation of the dyes studied using LC–APCI-MS (in PI and NI mode) and LC–ES-MS techniques.

2.4. Water analysis

Different drinking water volumes (500 and 300 ml) were spiked with several dyes, resulting in an analyte concentration of 0.6 ng/ml. The waters were acidified with acetic acid at different pH values (1.25 and 3).

The extraction method involved the Empore disk [poly(styrene–divinylbenzene) (PS–DVB)] that has been described previously [19,20]. A standard Millipore 47 mm filtration apparatus was used. The membrane extraction disks were manufactured by 3 M (St. Paul, MN, USA) under the trademark, Empore, and were distributed by J.T. Baker (Deventer, Netherlands). The disks used in these experiments were 47 mm in diameter and 0.5 mm thick. Each disk contains about 500 mg of PS–DVB.

Table 2
Gradient programme

Time (min)	Flow (ml/min)	%A[a]	%B[b]	Curve[c]
Initial	0.3	90	10	
5	0.3	90	10	6
20	0.3	40	60	6
23	0.3	40	60	6
30	0.3	0	100	6

[a]0.1 *M* ammonium acetate.
[b]Methanol.
[c]Linear gradient.

3. Results and discussion

3.1. General considerations

The first aim of this study was to determine a whole group of polysulphonated azo dyes that traditionally caused problems, using LC–MS techniques. LC–TS-MS was used and the information obtained is indicated in Table 7. Poor structural information was obtained under PI and NI TS-MS, as also reported by others [5–10], as well as poor sensitivity; the LOD in flow injection analysis is in the range of 4000 ng. This is the reason that some authors used

Table 3
Ions selected and time-scheduled SIM conditions

Compound	ES		APCI			
			NI		PI	
	m/z	Acquisition window (min)	*m/z*	Acquisition window (min)	*m/z*	Acquisition window (min)
Acid Red 1	464	19–23	231	4–9	466	4–9
	232	19–23	464	4–9	424	4–9
Acid Red 9	203	19–23	316	0–4	247	0–4
	225	19–23	451	0–4	453	0–4
Acid Red 13	228	23–30	236	16–21	158	16–21
	479	23–30	298	16–21	297	16–21
			350	16–21	299	16–21
					379	16–21
Acid Red 14	228	23–30	236	16–21	158	16–21
	479	23–30	298	16–21	297	16–21
			350	16–21	299	16–21
					379	16–21
Acid Red 73	511	23–30	197	16–21	198	16–21
	150	23–30	431	16–21	433	16–21
	255	23–30	350	16–21		
Mordant Yellow 8	401	23–30	172	9–16	251	9–16
	178	23–30	356	9–16	175	9–16
Acid Yellow 23	198	0–19	172	0–4	218	0–4
	211	0–19	198	0–4		
Direct Yellow 28	317	30–37	319	21–30	241	21–30
	318	30–37	321	21–30		
Mordant Black 11	266	0–19	318	4–9	173	4–9
	294	0–19	266	4–9		
Mordant Black 17	221	0–19	165	0–4	167	0–4
	249	0–19	260	0–4		
Acid Blue 113	317	30–37	298	21–30	231	21–30
	318	30–37	313	21–30	159	21–30

LC–MS–MS to better characterize the dyes [5,8,11–14]. It was reported that the concentration of ammonium acetate is a critical parameter under TS-MS for the characterization of various sulphonated azo dyes [6]. It was observed that amounts of ammonium acetate larger than 0.01 *M* produced a suppression of the response in TS-MS mode. The major ionization process in these dyes is anion evaporation of the analyte directly from the droplet; if too high a concentration of ammonium acetate is added, ejection of the more volatile acetate ion will compete with the evaporation of the dye anion. Something similar was noticed in the analysis of carbamate pesticides [21], i.e., the concentration of ammonium acetate influenced the response of TS and could suppress the signal intensity, in the relative and absolute sense. For this reason, the concentration of ammonium acetate was carefully investigated with all of the techniques studied and it was found to influence the signal intensity. Table 1 shows the concentration of optimized ammonium acetate concentration for each technique. This table includes

Table 4
Calibration data obtained with LC–ES-MS in time-scheduled SIM–NI mode for the dyes studied

Compound	*m/z*	Calibration equation	R^2	Linear range (ng)	LOD (ng)	LOQ (ng)
Acid Red 1	464	$y=-6128.8+4336.6x$	0.989	20–600	20	60
	232	$y=-818.7+1700.4x$	0.966	60–600	60	150
Acid Red 13	228	$y=6040+11717x$	0.996	3–900	3	11
Acid Red 14	228	$y=14257.8+3810.2x$	0.983	3–800	3	11
Acid Red 73	511	$y=-29605.2+20762.9$	0.984	12–800	12	50
Mordant Yellow 8	401	$y=-35766.5+24110.3x$	0.991	12–800	12	45
Acid Yellow 23	211	$y=-3752.5+1873.9$	0.995	76–800	76	180
Direct Yellow 28	317	$y=23062.1+5517.3x$	0.987	1.4–800	1	5
	318	$y=6043.6+1657.7x$	0.988	2.6–800	3	10
Mordant Black 11	266	$y=-2392.5+5286.9x$	0.997	13–800	13	30
	294	$y=2691.1+971.1x$	0.992	26-–800	26	80
Mordant Black 17	221	$y=-10599.1+4263.7$	0.991	70–700	70	160
	249	$y=-1926.4+989x$	0.996	70–700	70	160
Acid Blue 113	317	$y=1638+18650.8x$	0.997	2–700	2	5
	318	$y=336.8+24575.8x$	0.995	2–700	2	5

Number of data points, $n=7$, except for A. Red 13, A. Yellow 23 and M. Black 11, where $n=5$.
Standard errors for the intercept and the slope varied from 50–100 and from 3–10%, respectively.
Mordant Red was not detected.

Table 5
Calibration data obtained with LC–APCI-MS in time-scheduled SIM–NI mode for the dyes studied

Compound	*m/z*	Calibration equation	R^2	Linear range (ng)	LOD (ng)	LOQ (ng)
Acid Red 13	236	$y=-6141.7+497.4x$	0.932	140–2000	140	550
	298	$y=3976.9+1174.2x$	0.996	70–2000	70	
	350	$y=-6903.2+1291.6x$	0.982	80–2000	80	240
Acid Red 14	236	$y=-2040.7+341.4x$	0.991	100–3200	100	550
	298	$y=598.8+838.0x$	0.960	70–3200	70	210
	350	$y=-3399.9+1048.5x$	0.991	70–3200	70	210
Acid Red 73	197	$y=1458.6+562.5x$	0.994	60–2100	60	200
	431	$y=-1937+610.8x$	0.983	60–2000	60	200
	350	$y=4214.9+855.5x$	0.941	60–2000	60	200
Acid Yellow 23	172	$y=6591.4+1075.2x$	0.937	50–2000	50	150
Direct Yellow 28	319	$y=-14116.6+4484.2x$	0.923	50–2200	50	150
Mordant Black 17	165	$y=-963015+22726.3x$	0.934	700–2000	700	700
	260	$y=5108.9+413.9x$	0.946	70–2000	70	210
Acid Blue 113	298	$y=-6875.4+3772.8x$	0.860	70–2300	70	210
	313	$y=-9620.2+2126.3x$	0.916	120–2300	120	360

Number of data points, $n=7$, except for A. Red 13, Mordant Black 17 and A. Blue 113, where $n=5$.
Standard errors for the intercept and the slope varied from 100–200 and from 3–10%, respectively.
Acid Red 1, Mordant Red 9, Mordant Yellow 8 and Mordant Black 11 were not detected at the concentrations studied.

Table 6
Calibration data obtained with LC–APCI-MS in time-scheduled SIM–PI mode for the dyes studied

Compound	m/z	Calibration equation	R^2	Linear range (ng)	LOD (ng)	LOQ (ng)
Mordant Red 9	247	$y=5409.5+218.5x$	0.986	600–2600	600	1800
Acid Red 13	158	$y=-886.6+665.9x$	0.918	300–2000	300	2000
	297	$y=3211.6+231.2x$	0.973	800–2000	800	2400
Acid Red 14	158	$y=20822.3+1185.8x$	0.987	130–3200	130	800
	297	$y=25893.3+837.6x$	0.757	70–3200	70	210
	299	$y=17869.6+112.4x$	0.999	800–3200	800	2400
Acid Red 73	198	$y=87152.8+20634x$	0.988	30–2000	30	200
Acid Yellow 23	218	$y=-5415.5+735.1x$	0.981	240–2000	240	720
Direct Yellow 28	241	$y=-33352.3+4269x$	0.996	240–2200	240	1300
	321	$y=7313.1+213.75x$	0.987	800–2200	800	>2000
Acid Blue 113	231	$y=4284.3+2473x$	0.988	100–2300	100	400
	159	$y=20442.4+931.5x$	0.946	600–2300	600	1800

Number of data points, $n=7$, except for A. Red 13, A. Yellow 23, Direct Yellow 28 and A. Blue 113, where $n=5$.
Standard errors for the intercept and the slope varied from 50–150 and from 10–25%, respectively. The exception was A. Red 14, using the ion at m/z 299, which had standard errors for the intercept and the slope of below 1%.
Acid Red 1, Mordant Yellow 8, Mordant Black 11 and Mordant Black 17 were not detected at the concentrations studied.

other parameters that were optimized, such as the temperature of the source and the probe. The sulphonated azo dyes are very non-volatile compounds and it is necessary to use a high temperature for the source and the probe. We observed that when working at temperatures that were lower than those shown in Table 1, ionization of the dye did not take place and the probe could be easily blocked using all of the techniques, as could the cone of the source in ES and APCI mode, which made it necessary to clean the source every two–three days.

3.2. Mass spectral information

The fragment ions obtained in LC–TS-MS, LC–ES-MS and LC–APCI-MS mode for the polysulphonated azo dyes studied in this work are shown in Tables 7–9. From the data reported in these tables, it can be seen that APCI techniques show higher fragmentation than the other techniques. We noticed this phenomenon when analyzing organophosphorus pesticides [17]. Spectral information under TS conditions gave the $[M-Na]^-$ ion. The molecule loses one or two Na^+ atoms, depending on the number of Na atoms that it has, and replaces those atoms by hydrogen atoms. Usually when working in the NI mode, more sensitivity is observed, but there is not much difference between "filament on" or "filament off".

High flow pneumatically assisted ES gives, under NI mode, the $[M-2Na]^{2-}$ ion. With this technique, some fragment ions can be observed. Dyes like Mordant Red 9, Mordant Yellow 8 and Acid Yellow 23, all of which have a carboxylic group, lose this group and show the $[M-xNa-COO+H]^{2-}$ ion. In some dyes, other fragmentation ions, corresponding to a cleavage of the azo group near the naphthalic ring, can be observed.

In solution, the sulphonated azo dyes are ionized and since vaporization takes place from the solution in high flow ES-MS, 90% of the observed ions are due to ions present in solution [22]. This is the reason why we cannot obtain any peaks in the PI mode at this concentration.

APCI generally gives more structural information, this being its major difference from the other techniques. Cleavage of the azo linkage occurs in different ways, for example at the N-C bond, at the C-N bond of the remaining aromatic fragment, or at the double bond between the two atoms of the azo linkage. The same phenomenon was observed in fast atom bombardment (FAB) ionization [3,4].

All of the red dyes, except Acid Red 1, present cleavage of the azo group. For Acid Red 73, with two azo groups, the cleavage is produced in the azo

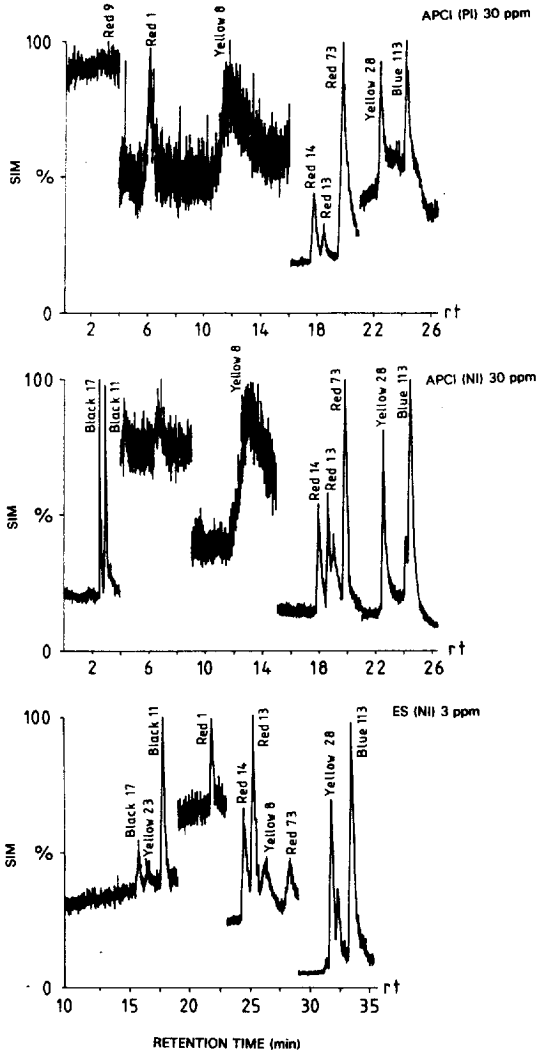

Fig. 2. LC–APCI-MS (PI, NI) and LC–ES-MS (NI) and time-scheduled SIM conditions of a mixture of dyes at 30 and 3 ppm, respectively. For a list of the ions monitored, see Table 4. For other experimental conditions, see Section 2.

group near the naphthalic ring. Fig. 3 shows the fragmentation scheme for this dye in the NI mode. Cleavage of the azo group can be observed, but so can cleavage of C-N group. Similar cleavage is observed by FAB MS [4].

One of the major differences between the data depicted in Tables 7–9 is the fragmentation observed under APCI-MS compared to that found with the other techniques. Such increased fragmentation is due to the losses of SO_3Na and $2SO_3Na$ for mono- and disulphonated azo dyes, respectively. In a previous paper [8], using TS, a loss of SO_3 was observed for most of the dyes studied and the polysulphonated azo dyes only lost two SO_3Na groups when these groups were attached to the same ring. When the SO_3Na groups were attached to different rings, the molecule could only lose one SO_3Na and two Na atoms. This is not the case in the example given in this paper. Acid Red 73 has two SO_3Na groups attached at the same group and Acid Red 14 has the two SO_3Na groups attached to different rings, however, both dyes lose the two SO_3Na groups. So it seems that the fact that the SO_3Na groups are attached to the same or different ring [8] is not the only reason. The disulphonated azo dyes, such as Acid Red 1, Mordant Red 9, Acid Yellow 23 and Acid Blue 113, only lose one SO_3Na group and for some reason, are not able to lose the second SO_3Na group. Apart from the fact that the SO_3 groups are attached to different rings, other reasons related to their chemical structure make the loss of the second SO_3Na group difficult. Acid Blue 113 was found to behave in a similar manner in this study, as was reported in a previous paper where APCI was used [14].

Acid Red 13 and Acid Red 14 are isomers and in LC–ES, no differences in their spectra can be observed, but in LC–APCI, there is a difference. For Acid Red 14, the peak corresponding to m/z 299 in PI (or 298 in NI) mode is an important peak (generally with a relative abundance (RA) of between 60–100), however, for Acid Red 13, this peak is not very important (RA between 10–50).

Mordant Yellow 8 and Acid Yellow 23, both of which have a pyrazolone ring, have important fragmentation patterns in negative mode. Azo cleavage and a pyrazolone cleavage ring were observed. The peak at m/z 198, corresponding to the isocyanate species $(O_3S-C_6H_4-N=C=O)^-$,is characteristic of the rupture of the pyrazolone ring. Loss of CO from 198 gave a peak at m/z 172. Fig. 4 shows the fragmentation obtained for Mordant Yellow 8 in NI mode.

Direct Yellow 28 gives an azo cleavage in both modes. It is a symmetrical molecule and the rupture of the azo group is favorable. For Acid Blue 113, cleavage of two azo groups can be observed.

Table 7
Typical fragment ions and relative abundance (RA) in LC–TS-MS in both PI and NI modes of operation

Compound	M_n [a]	PI			NI		
		Fragment ions	m/z	RA	Fragment ions	m/z	RA
Acid Red 1	509	$[MH-2Na+H+NH_4]^+$:	483	100	$[M-2Na+H]^{2-}$:	464	49
		$[MH-2Na+2H]^+$:	466	<5	$[M-Na]^-$:	486	100
		$[MH-Na+H]^+$:	488	82	$[M]^-$:	508	<5
		$[MH]^+$:	510	37			
		$[M+Na]^+$:	532	<5			
Mordant Red 9	518	$[MH-3Na+3H]^+$:	453	84	$[M-2Na]^{2-}$:	236	100
		$[MH-2Na+2H]^+$:	475	100	$[M-3Na+2H]^-$:	451	7
		$[MH-Na+H]^+$:	497	<5	$[M-2Na+H]^-$:	473	<5
		$[MH]^+$:	519	<5	$[M-Na]^-$:	495	<5
Acid Red 13	502	$[MH]^+$:	503	100	$[M-2Na]^{2-}$:	228	100
		$[M+Na]^+$:	525	59	$[M-2Na+H]^-$:	457	2
					$[M-Na]^-$:	479	83
Acid Red 14	502	$[MH-Na+H]^+$:	481	65	$[M-2Na]^{2-}$:	228	1000
		$[MH]^+$:	503	100	$[M-2Na+H]^-$:	457	4
		$[M+Na]^+$:	525	59	$[M-2Na]^-$:	479	19
Acid Red 73	556	$[MH-2Na+2H]^+$:	513	100	$[M-2Na+H]^-$:	511	100
		$[MH-Na+H]^+$:	535	50	$[M-Na]^-$:	533	2
		$[MH]^+$:	557	<5			
		$[M+Na]^+$:	579	<5			
Mordant Yellow 8	446	$[MH-2Na+2H]^+$:	403	100	$[M-2Na+H]^-$:	401	100
		$[MH-Na]^+$:	425	63	$[M-Na]^-$:	423	0
		$[MH]^+$:	447	33			
Acid Yellow 23	534	$[MH-Na+H]^+$:	513	100	$[M-3Na+2H]^-$:	467	66
		$[MH]^+$:	535	<5	$[M-Na+H]^-$:	489	78
		$[M+Na]^+$:	557	24	$[M-Na]^-$:	511	<5
					$[M-NaSO_3]^-$:	431	100
Direct Yellow 28	680	$[MH-2Na+2H]^+$:	637	51	$[M-2Na]^{2-}$:	317	100
		$[MH-Na]^+$:	659	51	$[M-2Na+H]^-$:	635	
		$[MH]^+$:	681	38			
Mordant Black 11	461	nd			nd		
Mordant Black 17	416	$[MH-Na+H]^+$:	395	100	$[M-Na]^-$:	393	100
		$[MH]^+$	417	<5	$[M]^-$:	415	70
		$[MH-NaSO_3+H]^+$:	315	<5	$[MH-NaSO_3]^-$:	313	30
Acid Blue 113	681	$[MH-2Na+2H]^+$:	638	100	$[M-2Na]^{2-}$:	317/318	100
		$[MH-Na]^+$:	660	4	$[M-2Na+H)^-$:	636	21
		$[MH]^+$	682	5	$[M-Na]^-$	658	13

The amount injected was 200 ppm.
[a] M_n=nominal mass.

Looking at the RA of the various spectra reported, we can see that in the case of APCI, variations in the RA were found after several months of operation. The range of RAs is indicated. This is related to the difficulties encountered with the analysis of these compounds and to the fact that the APCI heater was changed during this period. The new heater gave high fragmentation patterns and lower m/z ions were obtained. As indicated in Section 2, the APCI interface needs to be heated to a relatively high temperature (500°C) and, consequently, the heater may be damaged more easily. In addition, the interface needed to be cleaned more often than was reported for pesticide studies [17], since the dyes studied are much less volatile than organophosphorus pesticides. For high flow pneumatically assisted ES, no important changes in the RA of the various analytes were observed, and this is attributed to the fact that no heat is applied, so the non-volatile compounds are much less affected.

Table 8
Typical fragment ions and relative abundance (RA) using LC–ES-MS in the NI mode of operation

Compound	M_n	Fragment ions	m/z	RA
Acid Red 1	509	$[M-Na]^-$:	486	20 85
		$[M-2Na+H]^-$:	464	100
		$[M-Na]^{2-}$:	231/232	15
		$[H_2NC_{10}H_3(OH)(NHCOCH_3(SO_3)_2]^{2-}$	86	
Mordant Red 9	518	$[M-3Na+2H]^-$:	451	8
		$[M-3Na+H]^{2-}$:	225	100 100
		$[M-3Na-COO+H]^{2-}$:	203	
Acid Red 13	502	$[M-Na]^-$:	479	5
		$[M-2Na+H]^-$:	457	28
		$[M-2Na]^{2-}$	228	100
Acid Red 14	502	$[M-Na]^-$:	479	2.5
		$[M-2Na+H]^-$:	457	20
		$[M-2Na]^{2-}$:	228	100
Acid Red 73	556	$[M-Na]^-$:	533	10
		$[M-2Na+H]^-$:	511	8–100
		$[M-2Na]^{2-}$:	255	30
		Unknown	241	15
		$[H_2NC_{10}H_5(SO_3)_2]^{2-}$:	150/151	30–100
Mordant Yellow 8	446	$[M-Na]^-$:	423	8
		$[M-2Na+H]^-$:	401	20–100
		$[M-2Na]^{2-}$:	200	30–90
		$[M-2Na-COO+H]^{2-}$:	178	20–100
Acid Yellow 23	534	$[M-3Na+H)^{2-}$:	233	5–20
		$[M-3Na-COO+H]^{2-}$:	211	100
		$[OCNC_6H_4SO_3]^-$:	198	20
Direct Yellow 28	680	$[M-2Na]^{2-}$:	317	100
Mordant Black 11	461	Unknown	266	100
		Unknown	294	25
Mordant Black 17	416	Unknown	221	100
		Unknown	249	30
		Unknown	237	10
Acid Blue 113	681	$[M-2Na]^{2-}$:	317/318	100

The amount injected was 50 ppm.

4. Calibration

The various calibration equations using the different systems are reported in Tables 5–7. Several considerations should also be made. First of all, this is the first time that a complete calibration of various disulphonated azo dyes is given using LC–API-MS techniques and it indicates that quantitation is feasible, although in some instances, R^2 is less than 0.99. We have indicated the linear range of the different analytes and have shown various calibration graphs for some of the compounds. This is dependent on the ions that we select for calibration and we have indicated various possibilities in some cases, since various ions can be used and the RA may change.

The LODs and LOQs have been calculated in SIM mode. Table 3 shows the time-schedule used for each ion. From the data reported in Tables 4–6, it is clear that high flow pneumatically assisted ES offers the highest sensitivity for all of the analytes studied, except Acid Yellow 23 (about one order of magnitude lower than with APCI). Comparison of APCI with PI and NI modes shows that, in general, the NI mode is more sensitive than the PI mode.

The final comment is that only one of the dyes, Mordant Red 9, exhibits higher sensitivity with the PI mode than with the NI mode and high flow pneumatically assisted ES. The only reason for this could be the presence of COONa and OH groups attached to aromatic rings, giving the molecule a

Table 9
Typical fragment ions and relative abundance (RA) with LC–APCI-MS in the PI and NI modes of operation

Compound	M_n	PI			NI		
		Fragment ions	*m/z*	RA	fragment ions	*m/z*	RA
Acid Red 1	509	$[MH]^+$:	510	5	$[M-Na]^-$:	486	10
		$[MH-Na+H]^+$:	488	10	$[M-2Na+H]^-$:	464	10–100
		$[MH-2Na+2H]^+$:	466	70–100	$[M-2Na]^{2-}$:	231	0–100
		$[MH-2Na+H+NH_4]^+$:	483	30	$[M-2Na+2H-H_2O]^-$:	447	0–30
		$[MH-2Na+2H-H_2O]^+$:	448	80	$[m-2Na-COCH_3+3H]^-$:	423	0–40
		$[MH-2Na-COCH_3+3H]^+$:	424	25	$[M-2Na-COCH_3+H]^{2-}$:	210	70–100
Mordant Red 9	518	$[MH]^+$:	519	10	$[M-Na]^-$:	495	<5
		$[MH-Na+H]^+$:	497	5–30	$[M-2Na+H]^-$:	473	15
		$[MH-2Na+2H]^+$:	475	25–65	$[M-2Na+H]^{2-}$:	236	15
		$[MH-3Na+3H]^+$:	453	100	$[M-3Na+2H]^-$:	451	55–100
		$[MH-C_7O_2N_2H_4Na-NaSO_3+NH_2+2H]$:	263	0–40	$[M-C_7O_2N_2H_4Na-Na]^-$:	339/338	30–100
		$[MH-C_7O_2N_2H_4Na-NaSO_3+2H]^+$:	247	20–100	$[M-C_7O_2N_2H_4Na-2Na+H]^-$:	317/316	50–70
					[338−N+H]:	325	30–100
					[316−N+H]:	303	30–40
					$[C_{10}H_6OHSO_3]^-$:	223	10–30
Acid Red 13	502	$[MH]^+$:	503	10	$[M-Na]^-$:	479	20
		$[MH-NaSO_3+Na]^+$:	423	20	$[M-2Na+H]^-$:	457	5–40
		$[MH-2Na-SO_3+2H]^+$:	379	30–100	$[M-2Na-SO_3+H]^-$:	37	75–100
		$[MH-2Na-2SO_3+2H]^+$:	299/297	10–50	$[M-2Na-2SO_3]$:	298	5–60
		$[C_{10}H_7NHC_{10}H_7]$:	269	5–50	$[377-C_{10}OH_6+H]$:	236	100
			158	10–100	$[236-NH]^-$:	221	15–35
					$[HSO_3C_{10}H_6C_{10}H_6OH]$:	350	10–80
					$[HSO_3C_{10}H_7]$:	208	10–100
Acid Red 14	502	$[MH]^+$:	503	10	$[M-Na]^-$:	479	30
		$[MH-NaSO_3+Na]^+$:	423	15	$[M-2Na+H]^-$:	457	5–40
		$[MH-2Na-SO_3+2H]^+$:	379	10–60	$[M-2Na-SO_3+H]^-$:	377	5–100
		$[MH-2Na-2SO_3+2H]^+$:	299/297	20–−100	$[M-2Na-2SO_3]$:	298	40–100
		$[C_{10}H_7N=NC_{10}H_7]$:	282	30	$[377-C_{10}OH_6+H]$:	236	30–100
		$[C_{10}H_7NHC_{10}H_7]$:	269	35	$[236-NH]^-$:	221	20–60
			158	30–100	$[HSO_3C_{10}H_6C_{10}H_6OH]$:	350	10–45
					$[HSO_3C_{10}H_7]$:	208	25
Acid Red 73	556	$[MH]^+$:	557	5	$[M-Na]^-$:	533	0–70
		$[MH-Na+H]^+$:	535	15	$[M-2Na+H]^-$:	511	10–100
		$[MH-2Na+2H]^+$:	513	0–100	$[M-2Na-SO_3+H]^-$:	431	30–80
		$[MH-2Na-2SO_3+2H]^+$:	433	20	$[M-2Na-2SO_3+H]^-$:	350	0–50
		$[C_6H_5N=NC_6H_4NH_3]^+$:	198	60–100	Unknown	366	0–70
		$[C_6H_5N=NC_6H_5+H]^+$:	183	8–20	$[HN=NC_{10}H_5(SO_3H)_2]$:	316	10
					$[HN=NC_{10}H_5(SO_3H)]$:	236	20
					$[C_6H_5N=NCH_4NH_2]$:	197	15–30
Mordant Yellow 8	446	$[MH]^+$:	447	10	$[M-Na]^-$:	423	10
		$[MH-Na+H]^+$:	425	15	$[M-2Na+H]^-$:	401	15–50
		$[MH-2Na+2H]^+$:	403	10–100	$[M-2Na-COO+H]^-$:	355/356	50–100
		Unknown	251	0–100	$[401-C_6H_4COON_2]^-$:	253	25–100
		Unknown	221	0–50	$[356-C_6H_5N]^-$:	266	30–100
		Unknown	175	0–40	Unknown	329	0–40
					$[OCNC_6H_4SO_3]^-$:	198	0–10
					Unknown	182	0–80
					$[H_2NC_6H_4SO_3]^-$:	172	30–100
Acid Yellow 23	534	$[MH-Na+H]^+$:	513	5	$[M-3Na+2H]^-$:	468	10
		$[MH-2Na+2H]^+$:	491	5	$[M-COONa-2Na+2H]^-$:	423	10

Table 9 (*continued*)

Compound	M_n	PI			NI		
		Fragment ions	*m/z*	RA	fragment ions	*m/z*	RA
		$[MH-3Na+3H]^+$:	469	10	$[OCNC_6H_4SO_3]^-$:	198	15–30
		$[C_6H_3NCOC(NH)C(COOH)N+H]^+$:	218	100	$[H_2NC_6H_4SO_3]^-$:	172	100
					$[SO_3C_6H_4NC(OH)=C(HH_2)CH=N]$:	252/254	15–30
Direct Yellow 28	680	$[MH-2Na+2H]^+$:	637	10	$[M-Na]^-$:	657	5
		$[MH-2Na-2SO_3+2H]^+$:	557	10	$[M-2Na+H]^-$:	635	10
		$[CH_3C_6H_2SO_3NaSNCC_6H_4NH_2+H]^+$:	343	30	$[M-2Na-2SO_3+H]^-$:	555	10
		$[CH_3C_6H_2SO_3NaSNCC_6H_4NH_2+Na]^+$:	365	0–15	Unknown	401	20
		$[CH_3C_6H_2SO_3HSNCC_6H_4NH_2+H]^+$:	321	0–40	$[CH_3C_6H_2SO_3HSNCC_6H_4NH_2-H]^-$:	319	100
		$[CH_3C_6H_2HSNCC_6H_4NH_2+H]^+$:	241	100	[319−N]:	305	15
		Unknown	257	15–25			
Mordant Black 11	461	Unknown	313	60	Unknown	318	60
		Unknown	300	75	Unknown	294	50
		$[HSO_3C_{10}H_4OHNO_2NH_2]^+$:	286	10	Unknown	273	60
		Unknown	272	20	Unknown	266	60
		$[C_{10}H_6OHNH_2]^+$:	173	100	Unknown	175	100
					Unknown	160	80
Mordant Black 17	416	Unknown	391	20	Unknown	179	5
		Unknown	349	20	Unknown	165	100
		Unknown	259	20–30			
		Unknown	211	30–50			
		Unknown	189	30			
		Unknown	167	100			
Acid Blue 113	681	$[C_{10}H_6SO_3HC_6H_5+H]^+$:	300	90	$[M-2Na+H]^-$:	636	0–5
		Unknown	313	60	$[M-Na]^-$:	658	0–5
		$[NaO_3SC_6H_4N_2H+Na]^+$:	231	75	$[H_2NC_{10}H_5SO_3C_6H_5]^-$:	313	20–100
		$[NaO_3SC_6H_4NH_2+Na]^+$:	218	80	$[C_{10}H_6SO_3C_6H_5]^-$:298	80–100	
		$[HO_3SC_6H_5+H]^+/[H_2NC_{10}H_6NH_3]^+$:	159	100	$[O_3SC_6H_4NH_2]^-$:	17240–80	

The injected amount was 100 ppm.

much more basic character, despite the presence of the two SO_3Na groups. The fact that, in these experiments, LC–APCI-MS using the PI mode gives much better sensitivity than found in previous studies where disulphonated azo dyes were undetectable [14], can be attributed to better nebulization of the APCI interface. We did not observe a 20–50 fold poorer sensitivity for disulphonated azo dyes compared to monosulphonated azo dyes, as reported in reference [14], where APCI was used. This is also related to the design of the nebulizer in the present system.

4.1. Water analysis

Volumes of water [500 ml (at pH 1.25 and 3) and 300 ml (at pH 1.25)] were spiked with Acid Red 13, Acid Red 73, Mordant Yellow 8, Direct Yellow 8, Mordant Black 17 and Acid Blue 113 at 0.6 ng/ml. These waters were preconcentrated on C_{18} Empore disks and the dyes were collected with 2×10 ml of methanol. After careful evaporation of the methanol, 500 μl of water were added and 20 μl were injected onto the LC–ES-MS system, using SIM conditions. The recoveries were obtained from a standard containing 5 ng of the selected dyes, although the quantities injected were 12 and 7 ng for 500 and 300 ml of spiked water, respectively. Table 10 shows the results obtained for Acid Red 13, Direct Yellow 28 and Acid Blue 113. Other dyes were not sensitive at these low concentrations (see Table 4). In general, the recoveries obtained are poor and need to be optimized using other sorbent materials and experimental conditions. However, the techniques developed in this paper will permit the achievement of promising results for the extraction of disulphonated azo dyes from water samples.

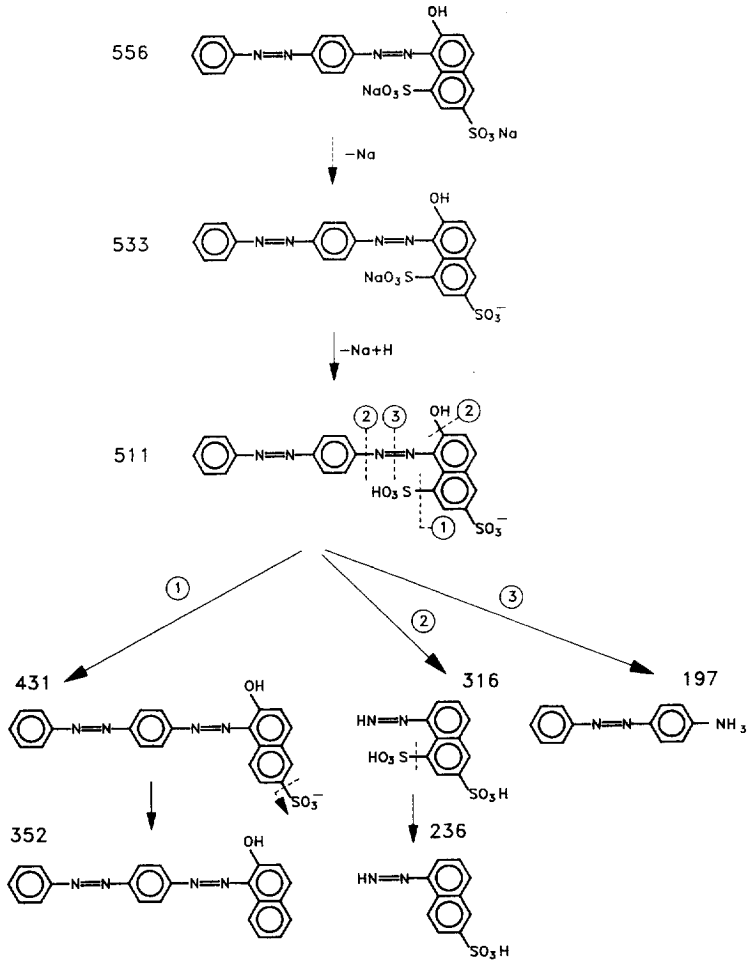

Fig. 3. Scheme of the fragmentation pattern obtained with APCI-MS in the NI mode for Acid Red 73.

5. Conclusions

A comparison between various API interfacing systems for the determination of polysulphonated azo dyes was performed. To our knowledge, this is the first time that a study has been carried out using various LC–MS interfaces for the determination of a variety of disulphonated azo dyes, due to the difficulties encountered in previous work using the LC–MS system. From the various techniques used, high flow pneumatically assisted ES gave the best performance in terms of sensitivity and reproducibility, although the structural information was poor, with losses of Na and 2Na. The use of APCI, in NI mode, although less sensitive than ES by approximately one order of magnitude, gives abundant structural information with losses of one or two SO_3Na groups. APCI in the PI mode, although somewhat less sensitive than in the NI mode for most of the dyes, offers better sensitivity for the monosulphonated azo dye, Mordant Red 9. The other question to take into consideration when using APCI-MS is the variability observed in the relative abundances of various fragments of the dyes, from 5–50 or 10–100 RA. This was attributed to the difficulty involved in ionizing the dyes with the APCI-MS system and to the high temperature of the APCI heater (500°C). In addition, the heater needed to be replaced several times, causing the variation observed, which did not occur with the ES system. Another way in which our

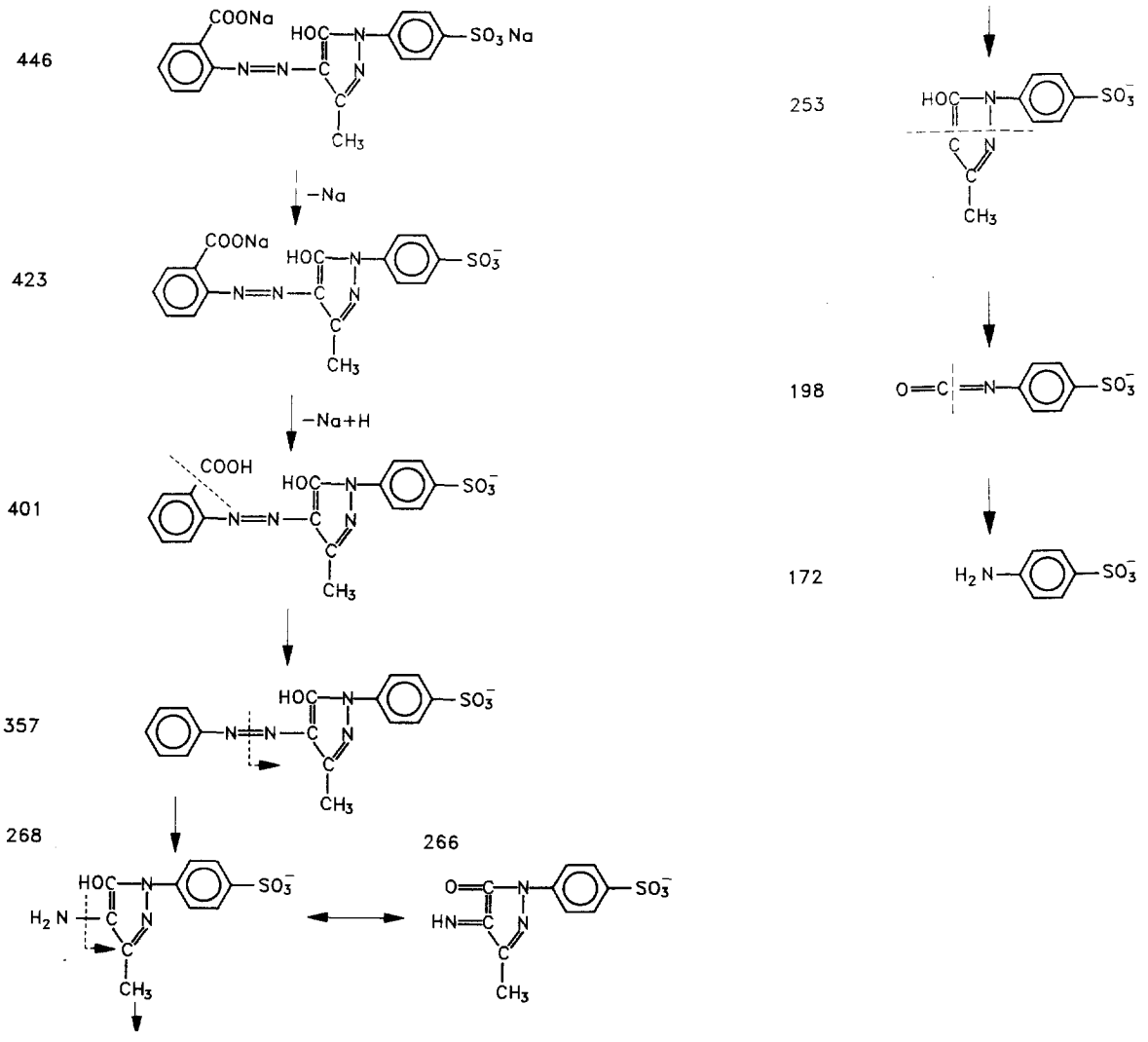

Fig. 4. Scheme of the fragmentation pattern obtained with APCI-MS in the NI mode for Mordant Yellow 8.

results differed from those published previously was that we did not observe a 20–50 decrease in sensitivity for disulphonated azo dyes compared with monosulphonated azo dyes. The application of the LC–MS approach to water analysis containing dyes still needs further improvement, although Acid Red 13, Direct Yellow 28 and Acid Blue 113 could be recovered from water samples spiked at the 0.6 ng/ml level. Since the analysis of polysulphonated azo dyes in water remains a problem that still presents difficulties, various extraction methods will be tested in the near future and used in combination with the present method as a routine method for monitoring disulphonated azo dyes in water samples.

Acknowledgments

This work was supported by the Commission of the European Communities Environment and Climate Program 1994–98 (Contract Number ENV4-

Table 10
Recoveries (%) with PS–DVB after extraction of dyes from water samples

Water volume (ml)	pH	Compounds					
		Red 13		Yellow 28		Blue 113	
		m/z	R (%)	*m/z*	R (%)	*m/z*	R (%)
500	1.25	228	nd	317	5	317	22.5
				318	nd	318	24.5
500	3	228	10	317	4	317	3.5
				318	4	318	4.5
300	1.25	226	nd	317	7	317	4
				318	6.5	318	7

R=recovery (%), *m/z* ions used for quantitation.

CT95_0016) and by CICYT (AMB96-1600-CE). C.R. acknowledges support from Rosi Alonso and Roser Chaler for technical assistance.

References

[1] M.S. Reich, Chem. Eng. News, 74 (1996) 10.
[2] E.J. Webwer, R.L. Adamas, Environ. Sci. Technol. 29 (1995) 1163.
[3] F. Ventura, A. Figueras, J. Caixach, J. Rivera, D. Fraisse, Org. Mass. Spectrom. 23 (1988) 558.
[4] F. Ventura, A. Figueras, J. Caixach, D. Fraisse, J. Rivera, Fresenius' Z. Anal. Chem. 335 (1989) 272.
[5] D. Barceló (Editor), Applications of LC–MS in Environmental Chemistry (Journal of Chromatography Library, Vol. 59), Elsevier, Amsterdam, 1996, Ch. 4.
[6] D.A. Flory, M.M. McLean, M.L. Vestal, L.D. Betowski, Rapid Commun. Mass Spectrom. 1 (1987) 48.
[7] M.A. McLean, R.B. Freas, Anal. Chem. 61 (1989) 2054.
[8] R. Straub, R.D. Voyksner, J.T. Keever, J. Chromatogr. 627 (1992) 173.
[9] J. Ynon, T.L. Jones, D.L. Betowski, Biomed. Environ. Mass Spectrom. 18 (1989) 445.
[10] A. Groeppelin, M.W. Linder, K. Schellenberg, H. Moser, Rapid Commun. Mass Spectrom. 5 (1991) 203.
[11] P.O. Edlund, E.D. Lee, J.D. Henion, W.L. Budde, Biomed. Environ. Mass Spectrom. 14 (1987) 343.
[12] J.A. Bellantrine, D. Games, S. Slater, Rapid Commun. Mass Spectrom. 9 (1995) 1403.
[13] H. Lin, R.D. Voyksner, Anal. Chem. 65 (1993) 451.
[14] A.P. Bruins, L.O.G. Weidolf, J.D. Henion, W.L. Budde, Anal. Chem. 59 (1987) 2647.
[15] C. Molina, M. Honing, D. Barceló, Anal. Chem. 66 (1994) 4444.
[16] S. Chiron, S. Papilloud, W. Haerdi, D. Barceló, Anal. Chem. 67 (1995) 1637.
[17] S. Lacorte, D. Barceló, Anal. Chem. 68 (1996) 2464.
[18] Colour Index, Society of Dyers and Colourists, Bradford, UK, 3rd ed., 2nd revision, 1982.
[19] S. Lacorte, C. Molina, D. Barceló, Anal. Chim. Acta 2811 (1993) 71.
[20] W.C. Brumley, C.M. Brownrigg, H.A. Grenige, J. Chromatogr. A 680 (1994) 635.
[21] M. Honing, D. Barceló, B.L.M. Van Barr, R.T. Ghijsen, U.A.Th. Brinkman, J. Am. Soc. Mass Spectrom. 5 (1994) 913.
[22] C. Molina, P. Grasso, E. Benfenati, D. Barceló, J. Chromatogr. A 737 (1996) 47.